# Improved Wald Transformation $p$-Chart For Nonconforming Fraction

Saichon Sinsomboonthong[1] and Juthaphorn Sinsomboonthong[2*]

[1] *Department of Statistics, School of Science, King Mongkut's Institute of Technology Ladkrabang, Bangkok 10520, Thailand*
[2] *Department of Statistics, Faculty of Science, Kasetsart University, Bangkok 10900, Thailand*
[*] *Corresponding author. E-mail: fscijps@ku.ac.th*

*Received: Jan. 11, 2024; Accepted: Apr. 15, 2024*

This study proposes a new improved transformation $p$-chart for nonconforming fraction of a production process, called improved Wald transformation $p$-chart. Via a simulation study, the efficiency of the proposed control chart was compared with the traditional p-chart, the improved square root transformation $p$-chart, and the Wilson $p$-chart. The simulation was conducted using the Monte Carlo technique for 180 situations and 10,000 times for each situation. The studied situations were as follows: the nonconforming fraction was set to be $0.01, 0.02, 0.05, 0.07$, and $0.09$ ; the shift of the nonconforming fraction was set to be $1.1, 1.3, 1.5, 2.0, 3.0$, and $4.0$; and the sample size (n) was set to be $30, 50, 100, 300, 500$, and $1000$ . The efficiency measures were out-of-control average run length and standard deviation of the run length. The results showed that the proposed chart was the most efficient among the four tested charts for a large sample size. In addition, the proposed chart tended to perform with the best efficiency for large sample sizes, $n \geq 500$, and small nonconforming fraction below 0.1. It performed well with all the tested shifts of nonconforming fraction. However, the sensitivity to detect out-of-control items in the production process seemed to be same among the tested charts for smaller sample size, $n < 500$.

**Keywords:** nonconforming fraction; p-chart; run length; transformation

http://dx.doi.org/10.6180/jase.202504_28(4).0010

## 1. Introduction

The success of a production process depends on factors and various steps that were specified from the beginning of the process. In addition, a good production process plan will help reduce costs and production time. It also reduces various risks in production and increases the ability to respond to customer needs more quickly. A good production process will help business to be successful and grow sustainably. Nowadays, manufacturing competition is quite high. Product quality plays an important role in consumer purchasing decision, i.e., product quality must meet consumer needs [1]. Many factors affect product quality, factors such as employees, machines, raw materials, etc. If these factors are proper and do not change with time, the product will meet the required quality [2–5]. Therefore, it is necessary to control the manufacturing process so that it meets the desired quality at low cost. Control chart is the most popular statistical process control (SPC) instrument for detection of abnormalities in production process [2–4]. If the process operator can quickly detect and solve an out-of-control process problem, the loss can be minimized. A widely used attribute control chart for detecting the fraction of nonconforming items in a production process is a nonconforming fraction control chart, usually called a $p$-chart. A problem with this chart is its slowness in detecting process changes [6–13]. Many studies have concluded that the traditional $p$-chart did not perform well. There have been several ways to improve $p$-chart. After it is improved, it should be more sensitive to detect process abnormalities when the nonconforming fraction in the process slightly changes from the target. In the past, $p$-chart was improved based on the idea of several kinds of transformations. Chen

[14] improved $p$-chart with simple adjustments to the control limits of the $p$-chart. He compared the efficiency of the improved $p$-chart, arcsine $p$-chart and Q chart and found that the improved $p$-chart and Q chart were efficient for large nonconforming fraction. In the real world, a small nonconforming fraction often occurs in the production process, so $p$-chart is not the appropriate tool [15, 16]. An improved square root transformation $p$-chart, ISRT $p$-chart, was proposed by Tsai et al. [15]. The efficiencies of four charts-exact $p$, modified $p$, regression-based $p$, and ISRT $p$-were compared via a numerical study. The ISRT $p$-chart and the exact $p$-chart performed with the same efficiency, adequate for a low level of nonconforming fraction. Later in 2014, Sukparungsee [12] found that ISRT p-chart performed well for the shift in nonconforming fraction of over 0.5 , the nonconforming fraction level $(p_0)$ of 0.05 and 0.1 , and the sample size $(n)$ of 50 and 70. In 2012, Anna and Caten [17] proposed a new control chart, a beta chart, for monitoring nonconforming fraction when data were taken from binomially distributed population. Their proposed control limits were derived based on the beta distribution which is an approximation to the binomial distribution. This distribution is more appropriate for values of the random variable between 0 and 1. The efficiency comparison was studied via a simulation of situations consisting of nonconforming fraction $(p_0)$ of $0.001, 0.01$, and $0.10$ ; sample size ( $n$ ) of 50, 200, 300, and 1500 ; and the shift of nonconforming fraction $(\delta)$ in production process of $0.001, 0.01$, and 0.02. The results show that the beta chart was more sensitive for process monitoring in terms of in-control $(ARL_0)$ and out-of-control $(ARL_1)$ average run lengths. In addition, this proposed chart is better than the classical chart [18] for monitoring nonconforming fractions. Furthermore, Rungruang [19] compared the efficiencies of three charts-Q chart, moving average $p$-chart, and beta chart-in monitoring nonconforming fractions. For an out-of-control process, the beta control chart was the most efficient for a small nonconforming fraction and a small shift in nonconforming fraction. However, the moving average $p$-chart was more suited for a large nonconforming fraction and a large shift in nonconforming fraction, regardless of the sample size. Two years later, Rod-o et al. [13] used the concept of adjusted Wald confidence interval estimation [20] to develop control limits of $p_{AC}$ chart for monitoring nonconforming fraction. They compared its efficiency with those of three charts: beta chart, moving average $p$-chart, and $p$-chart. The beta chart was the most effective for almost all levels of shift in nonconforming fraction and sample sizes when the nonconforming fraction was small. However, the moving average $p$-chart was more effective for a large nonconforming fraction. Furthermore, the proposed $p_{AC}$ chart provided a good performance for almost all nonconforming fractions and sample sizes when the shift in nonconforming fractions increased. In addition, Tsai et al. [15] proposed the ISRT $p$-chart and compared it with several other kinds of charts. Small sample sizes were required to obtain positive lower control limits for the ISRT $p$-chart. Numerical results indicate that the ISRT $p$-chart can match any specific percentile point of run length distribution of the true limit of an unknown parameter. Therefore, we followed the concept of this chart construction in developing our proposed chart. Another chart was derived based on Wilson confidence interval and proposed by Park [21], called Wilson $p$-chart. Park compared the efficiencies of $p$-chart, a modified $p$-chart by Chen [14], and Wilson $p$-chart. Wilson $p$-chart outperformed the other charts for small nonconforming fractions. In this research, data is taken to be analyzed for a short period of time while the investigation process was in progress. This was the focus of this study, so the progressive charts, which often took historical data into account, were not investigated, which is not a disadvantage because most progressive charts are complex and difficult to use in practice. Therefore, the main objective of this research was to develop a method for improving $p$-chart. The secondary objective was to compare it to other kinds of existing control charts.

An attribute control chart for monitoring nonconforming fraction in a production process is proposed. It is called an improved Wald transformation $p$-chart (IWT $p$-chart). The proposed control limits were derived based on the square root transformation concept and adjusted Wald confidence interval estimation concept [20]. Agresti and Coull [20] reported that the interval estimation of the proportion parameter for binomial distribution performed well for both small proportion parameter and sample size. Therefore, the authors hope that the proposed control chart would be more sensitive in detecting out-of-control values for small nonconforming fractions in a manufacturing process (of which this situation occurs frequently in practice). In addition, the efficiency of the proposed chart was compared to those of ISRT $p$-chart, Wilson $p$-chart, and $p$-chart in terms of out-of-control average run length $(ARL_1)$ and standard deviation of the run length $(SDRL)$. The authors of Khoo et al. [22], Chen et al. [23], and Khilare and Shirke [24], compared performances in terms of $ARL_1$ and SDRL. They found that no matter which measure was used, the analysis results were not different. Our contribution to the field is our proposed IWT $p$-chart that can control nonconforming fractions in a production process with the best efficiency for large sample sizes and small nonconforming fractions and outperforms several existing kinds of charts.

## 2. Materials and methods

This study proposes an IWT $p$-chart. In addition, its efficiency was compared to those of $p$-chart, ISRT $p$-chart and Wilson $p$-chart. These charts are explained below.

### 2.1. Nonconforming Fraction Control Chart (p-chart)

A well-known control chart for monitoring fractions of nonconforming was developed according to the general model of Shewhart [4]. It is called a nonconforming fraction control chart or $p$-chart. Let $p$ be the fraction of nonconforming items of a process. Let $X$ be the number of nonconforming items of the process that has a binomial distribution with parameters $n$ and $p$ ($n$ is the sample size, and $p$ is the nonconforming fraction). When the parameter $p$ is known, the process can be monitored by plotting the sample nonconforming fractions $\hat{p}_i = \frac{X_i}{n}$, where $i = 1, 2, \ldots, m$ on the $p$-chart with the center line, lower and upper control limits are given in Eq. (1).

$$CL_P = p, \quad LCL_P = p - L\sqrt{\frac{p(1-p)}{n}} \quad \text{and} \quad UCL_P = p + L\sqrt{\frac{p(1-p)}{n}} \tag{1}$$

where $L$ is the distance of the control limits from the center line. It is customary to choose $L = 3$ so that the in-control average run length $(ARL_0)$ was 370.4 and the probability of type I error was 0.0027 , i.e., an incorrect out-of-control signal or false alarm would be generated for only 27 out of 10,000 times. These limits are called three-sigma control limits. When the parameter $p$ is unknown, it can be estimated by the mean of nonconforming fraction from the samples and denoted by symbol $\bar{p}$, where $\bar{p} = \frac{\sum_{i=1}^{m} \hat{p}_i}{m}$ and $m$ is the number of samples with size $n$ that are taken from the process.

### 2.2. Improved Square Root Transformation $p$-Chart (ISRT $p$-chart)

In 2006, a new attribute control chart, namely, an improved square root transformation $p$-chart or the ISRT $p$-chart was proposed [15]. A square root transformation was used to construct the lower and upper control limits of the ISRT -p-chart. Let $X$ be a binomial random variable with parameters $n$ and $p$, where $n$ is the sample size, and $p$ is the nonconforming fraction of the process. The ISRT $p$-chart can be constructed with the center line as $CL_{\text{ISRT}_p} = f(p) = \sqrt{p}$. The lower $\left(LCL_{\text{ISRT}_p}\right)$ and upper $\left(UCL_{\text{ISRT}p}\right)$ control limits of the ISRT $p$-chart can be expressed as Eq. (2).

$$\begin{aligned} LCL_{\text{ISRT}_p} &= \sqrt{p} - L\left(\frac{1}{2\sqrt{p}}\right)\sqrt{\frac{p(1-p)}{n}} + \frac{1}{2}\left(-\frac{1}{4p\sqrt{p}}\right)\left(\frac{9p(1-p)}{n}\right) \\ &= \sqrt{p} - \frac{L}{2}\sqrt{\frac{1-p}{n}} - \frac{9}{8}\left(\frac{1-p}{n\sqrt{p}}\right) \\ UCL_{\text{ISRT}p} &= \sqrt{p} + L\left(\frac{1}{2\sqrt{p}}\right)\sqrt{\frac{p(1-p)}{n}}. + \frac{1}{2}\left(-\frac{1}{4p\sqrt{p}}\right)\left(\frac{4p(1-p)}{n}\right) \\ &= \sqrt{p} + \frac{L}{2}\sqrt{\frac{1-p}{n}} - \frac{1}{2}\left(\frac{1-p}{n\sqrt{p}}\right) \end{aligned} \tag{2}$$

where $L$ is the distance of the control limits from the center line. If three-sigma control limits are taken, then $L$ equals 3 for asymptotically standard normal distribution. The parameter $p$ can be estimated from the mean of nonconforming fractions in the samples and is denoted by symbol $\bar{p}$, where $\bar{p} = \frac{\sum_{i=1}^{m} \hat{p}_i}{m}$. The plot statistic of nonconforming fractions for the ISRT $p$-chart is given by $f(\hat{p}_i) = \sqrt{\frac{X_i}{n}}$, where $X_i$ is the number of nonconforming items from the $i^{\text{th}}$ subgroup for $i = 1, 2, \ldots, m$, and $n$ is the sample size.

### 2.3. Improved $p$-Chart Based on the Wilson Interval (Wilson p-chart)

In 2013, Park [21] proposed Wilson p-chart based on the Wilson confidence interval concept. Its performance is superior to those of several existing kinds of charts in terms of how close its coverage probabilities are to the given confidence coefficient [20]. It was found that Wilson $p$-chart outperformed the conventional $p$-chart and a modified $p$-chart proposed by Chen [14], especially for small values of nonconforming fractions. Let $X_i$ be the number of nonconforming items in the $i^{\text{th}}$ subgroup of sample size $n$ from the production process, and let it have a binomial distribution with parameters $n$ and $p$, where $p$ is the nonconforming fraction of the process. When the parameter $p$ is unknown, it can be estimated by the pooled mean of nonconforming fraction as $\bar{p} = \frac{\sum_{i=1}^{m} \hat{p}_i}{m}$, where $m$ is the number of samples with size $n$ that are taken from the process. The process can be monitored by plotting the sample nonconforming fractions $\hat{p}_i = \frac{X_i}{n}$, where $i = 1, 2, \ldots, m$ on the Wilson $p$-chart. Then, plot the lower $\left(LCL_{\text{Wilson }p}\right)$ and upper $\left(UCL_{\text{Wilson }p}\right)$ control limits of the Wilson $p$-chart, which can be expressed as Eqs. (3) and (4), respectively,

$$LCL_{\text{Wilson } p} = \frac{\bar{p} + k^2/(2N)}{1 + k^2/N} - \frac{k}{1 + k^2/N}\sqrt{\frac{\bar{p}(1-\bar{p})}{n} + \frac{k^2}{4nN}} \quad (3)$$

$$UCL_{\text{Wilson } p} = \frac{\bar{p} + k^2/(2N)}{1 + k^2/N} + \frac{k}{1 + k^2/N}\sqrt{\frac{\bar{p}(1-\bar{p})}{n} + \frac{k^2}{4nN}} \quad (4)$$

where $N = mn$. The target of $ARL_0$ was approximately 370.4, hence $k = 3$ was assigned for the construction of these control limits with the standard normal quantile.

### 2.4. Proposed Control Chart

The attribute control chart for nonconforming fraction of the process, namely, the improved Wald Transformation $p$-chart or IWT $p$-chart is proposed. This proposed chart was based on two concepts: the concept of transformation of ISRT $p$-chart and the concept of adjusted Wald confidence interval estimation [20]. Because a small nonconforming fraction (p) in binomial distribution often occurs in a process, the normal approximation of binomial distribution cannot approximate it adequately [15, 25–27]. Hence, an improved square root transformation procedure of Tsai et al. [15] was used to construct the proposed control chart. Furthermore, the efficiency of adjusted Wald confidence interval estimation of proportion parameter for the binomial distribution performed well for a small proportion parameter and a small sample size. Therefore, these two concepts were considered in finding the lower and upper limits of the proposed chart. Let a random variable $X$ be the number of nonconforming items in a process that has a binomial distribution with parameters $n$ and $p$, where $n$ is a sample size and $p$ is the nonconforming fraction. If most values of $X$ are equal to 0 , then the transformation in the form of $\sqrt{X}$ is less accurate because the range of low-mean transformed values may be greater than the range of high-mean transformed values. Therefore, before applying the square root transformation of $X$, two successes and two failures for each sample was added to the dataset [20]. That is, the point estimator of $p$ is given by $\hat{p}_{Adj} = \frac{X+2}{n+4}$, and this is the adjustable nonconforming fraction from the sample of size $n$.

**Definition 1:** Let $f(x)$ be a real-value function that is infinitely differentiable at point $x = a$, then the Taylor series of function $f(x)$ at the point $a$ is given by Eq. (5),

$$f(a) + \frac{f'(a)}{1!}(x-a) + \frac{f''(a)}{2!}(x-a)^2 + \frac{f'''(a)}{3!}(x-a)^3 + \ldots = \sum_{n=0}^{\infty} \frac{f^{(n)}(a)}{n!}(x-a)^n \quad (5)$$

where $f^{(n)}(a)$ denotes the $n^{\text{th}}$ derivative of $f$ at the point $a$. The Taylor series of function $f(x)$ at the point $a = 0$ is called a Maclaurin series for $f(x)$ [28].

**Theorem 1:** Let $X$ be the number of nonconforming items of a process that has a binomial distribution with parameters $n$ and $p$. Let $\hat{p}_{Adj}$ be the nonconforming fraction from the sample of size $n$. If $f\left(\hat{p}_{Adj}\right) = \sqrt{\hat{p}_{Adj}}$ is a function of the nonconforming fraction from the samples, then $\sqrt{n}\left[f\left(\hat{p}_{Adj}\right) - f(p) - \frac{f''(p)}{2}\left(\hat{p}_{Adj} - p\right)^2\right]$ and $f'(p)\sqrt{n}\left(\hat{p}_{Adj} - p\right)$ have the same limit distribution.

**Proof:** Suppose $f\left(\hat{p}_{Adj}\right) = \sqrt{\hat{p}_{Adj}}$ is a function of the nonconforming fraction from samples of size $n$. By definition 1, using the Taylor series for function $f\left(\hat{p}_{Adj}\right)$ to the second order at the point, $\hat{p}_{Adj} = p$, then $f\left(\hat{p}_{Adj}\right)$ is given by

$$f\left(\hat{p}_{Adj}\right) \cong f(p) + f'(p)\left(\hat{p}_{Adj} - p\right) + \frac{f''(p)}{2}\left(\hat{p}_{Adj} - p\right)^2$$

or

$$f\left(\hat{p}_{Adj}\right) - f(p) - \frac{f''(p)}{2}\left(\hat{p}_{Adj} - p\right)^2 \cong f'(p)\left(\hat{p}_{Adj} - p\right)$$

Hence,

$$\sqrt{n}\left[f\left(\hat{p}_{Adj}\right) - f(p) - \frac{f''(p)}{2}\left(\hat{p}_{Adj} - p\right)^2\right] \cong f'(p)\sqrt{n}\left(\hat{p}_{Adj} - p\right)$$

and $\sqrt{n}\left[f\left(\hat{p}_{Adj}\right) - f(p) - \frac{f''(p)}{2}\left(\hat{p}_{Adj} - p\right)^2\right]$ and $f'(p)\sqrt{n}\left(\hat{p}_{Adj} - p\right)$ are the same formula and they have the same limit distribution.

**Definition 2:** Let $X$ be a random variable that has a binomial distribution with parameters $n$ and $p$. Then, $x$ has an approximated normal distribution with a mean $E(X) = \mu = np$ and variance $V(X) = \sigma^2 = np(1-p)$ for a sufficient large sample size and $p$ close to 0.5 [29, 30].

By definition 2, the binomial distribution will tend to be positively or negatively skewed when $np$ close to 0 or 1 , but it will approximate a normal distribution for a large sample size [29].

**Lemma 1:** Let $X$ be the number of nonconforming items of a process that has a binomial distribution with parameters $n$ and $p$. For a sufficiently large sample size, the sampling distribution of $\hat{p}_{Adj} = \frac{X+2}{n+4}$ approximates a normal distribution with a mean of $\mu_{\hat{p}_{Adj}} = \frac{np+2}{n+4}$ and a variance of $\sigma^2_{\hat{p}_{Adj}} = \frac{np(1-p)}{(n+4)^2}$.

**Proof:** Suppose $X$ is a random variable that has a binomial distribution with parameters $n$ and $p$. The sample nonconforming fraction is given by $\hat{p}_{Adj} = \frac{X+2}{n+4}$. By definition 2, the mean and variance of $\hat{p}_{Adj}$ can be derived as Eqs. (6) and (7), respectively,

$$\begin{aligned}\mu_{\hat{p}_{Adj}} &= E\left(\hat{p}_{Adj}\right) = E\left(\frac{X+2}{n+4}\right) = \frac{1}{n+4}E(X+2) \\ &= \frac{1}{n+4}\{E(X)+2\} = \frac{np+2}{n+4}\end{aligned} \tag{6}$$

$$\begin{aligned}\sigma^2_{\hat{p}_{\text{Adj}}} &= V\left(\hat{p}_{Adj}\right) = V\left(\frac{X+2}{n+4}\right) = \frac{1}{(n+4)^2}V(X+2) \\ &= \frac{1}{(n+4)^2}V(X) = \frac{np(1-p)}{(n+4)^2}\end{aligned} \tag{7}$$

By the central limit theorem, the sampling distribution of $\hat{p}_{Adj} = \frac{X+2}{n+4}$ approximates a normal distribution with a mean of $\mu_{\hat{p}_{Adj}} = \frac{np+2}{n+4}$ and a variance of $\sigma^2_{\hat{p}_{Adj}} = \frac{np(1-p)}{(n+4)^2}$ for a sufficiently large sample size.

**Theorem 2:** Let $X$ be the number of nonconforming items of a process that has a binomial distribution with parameters $n$ and $p$. The nonconforming fraction of a sample is expressed as $\hat{p}_{Adj} = \frac{X+2}{n+4}$. Since $f(p) = \sqrt{p}$, $f'(p)\sqrt{n}\left(\hat{p}_{Adj} - p\right)$ is approximately normally distributed with a mean of $\frac{f'(p)\sqrt{n}(np+2)}{n+4} - f'(p)\sqrt{n}p$ and a variance of $\frac{[f'(p)]^2 n^2 p(1-p)}{(n+4)^2}$ for a sufficiently large sample size.

**Proof:** Suppose $X$ is a random variable that has a binomial distribution with parameters $n$ and $p$. The nonconforming fraction of a sample is given by $\hat{p}_{Adj} = \frac{X+2}{n+4}$ and $f(p) = \sqrt{p}$. By Lemma 1, $\hat{p}_{Adj} = \frac{X+2}{n+4}$ is approximately normally distributed with a mean of $E\left(\hat{p}_{Adj}\right) = \frac{np+2}{n+4}$ and a variance of $V\left(\hat{p}_{Adj}\right) = \frac{np(1-p)}{(n+4)^2}$ for a sufficiently large sample size. The mean and variance of $f'(p)\sqrt{n}\left(\hat{p}_{Adj} - p\right)$ are expressed as Eqs. (8) and (9), respectively,

$$\begin{aligned}E\left[f'(p)\sqrt{n}\left(\hat{p}_{Adj} - p\right)\right] &= f'(p)\sqrt{n}E\left(\hat{p}_{Adj} - p\right) \\ &= f'(p)\sqrt{n}\left[E\left(\hat{p}_{Adj}\right) - p\right] \\ &= f'(p)\sqrt{n}\left[\left\{\frac{np+2}{n+4}\right\} - p\right] \\ &= \frac{f'(p)\sqrt{n}(np+2)}{n+4} - f'(p)\sqrt{n}p\end{aligned} \tag{8}$$

$$\begin{aligned}V\left[f'(p)\sqrt{n}\left(\hat{p}_{Adj} - p\right)\right] &= \left[f'(p)\right]^2 nV\left(\hat{p}_{Adj} - p\right) \\ &= \left[f'(p)\right]^2 nV\left(\hat{p}_{Adj}\right) \\ &= \left[f'(p)\right]^2 n\left[\frac{np(1-p)}{(n+4)^2}\right] \\ &= \frac{\left[f'(p)\right]^2 n^2 p(1-p)}{(n+4)^2}\end{aligned} \tag{9}$$

By the central limit theorem, the distribution of $f'(p)\sqrt{n}\left(\hat{p}_{Adj} - p\right)$ is approximately normally distributed with a mean of $\frac{f'(p)\sqrt{n}(np+2)}{n+4} - f'(p)\sqrt{n}p$ and a variance of $\frac{[f'(p)]^2 n^2 p(1-p)}{(n+4)^2}$ for a sufficiently large sample size.

**Theorem 3:** Let $e = \left|\hat{p}_{Adj} - p\right|$ be the absolute error for the estimation of $p$ with $\hat{p}_{Adj} = \frac{X+2}{n+4}$ and $f(p) = \sqrt{p}$. The center line and the lower and upper bounds of three-sigma control limits for the IWT $p$-chart are given by $CL_{\text{IWT}p} = f(p) = \sqrt{p}$,

$$\begin{aligned}LCL_{\text{IWT}p} = \frac{\sqrt{p}}{2} - \frac{3\sqrt{n(1-p)}}{2(n+4)} + \frac{np+2}{2(n+4)\sqrt{p}} \\ - \frac{25n(1-p)}{8\sqrt{p}(n+4)^2}\end{aligned}$$

$$\begin{aligned}UCL_{\text{IWT}p} = \frac{\sqrt{p}}{2} + \frac{3\sqrt{n(1-p)}}{2(n+4)} + \frac{np+2}{2(n+4)\sqrt{p}} \\ - \frac{2n(1-p)}{\sqrt{p}(n+4)^2}\end{aligned}$$

By theorem 3, the parameter $p$ can be estimated as the mean of nonconforming fraction of a sample and denoted by symbol $\bar{p}_{Adj} = \frac{\sum_{i=1}^{m}\hat{p}_{Adj_i}}{m}$, where $\hat{p}_{Adj_i} = \frac{X_i+2}{n+4}$ for $i = 1,2,\ldots,m$. The plot statistic of nonconforming fraction for the IWT $p$-chart is given by $f\left(\hat{p}_{Adj_i}\right) = \sqrt{\frac{X_i+2}{n+4}}$, where $X_i$ is the number of nonconforming items from the i$^{\text{th}}$ subgroup and $n$ is the sample size.

**Proof:** Let $e = \left|\hat{p}_{Adj} - p\right|$ be the absolute error for the estimation of $p$ with $\hat{p}_{Adj} = \frac{X+2}{n+4}$ and $f(p) = \sqrt{p}$. By Theorem 1 and Theorem 2, consider the standardized form of $f'(p)\sqrt{n}\left(\hat{p}_{Adj} - p\right)$ or $\sqrt{n}\left[f\left(\hat{p}_{Adj}\right) - f(p) - \frac{f''(p)}{2}\left(\hat{p}_{Adj} - p\right)^2\right]$. It is

$$\begin{aligned}Z &= \frac{(n+4)\sqrt{n}\left[f\left(\hat{p}_{Adj}\right) - f(p) - \frac{f''(p)}{2}e^2\right]}{|f'(p)|\,n\sqrt{p(1-p)}} \\ &\quad - \frac{\left(f'(p)\sqrt{n}(np+2) - (n+4)f'(p)\sqrt{n}p\right)}{|f'(p)|\,n\sqrt{p(1-p)}} \\ &= \frac{(n+4)\left[f\left(\hat{p}_{Adj}\right) - f(p) - \frac{f''(p)}{2}e^2\right]}{|f'(p)|\sqrt{np(1-p)}} \\ &\quad - \frac{(np+2)}{\sqrt{np(1-p)}} + \frac{(n+4)p}{\sqrt{np(1-p)}}\end{aligned}$$

The distribution of $\frac{(n+4)\left[f(\hat{p}_{Adj})-f(p)-\frac{f''(p)e^2}{2}\right]}{|f'(p)|\sqrt{np(1-p)}} - \frac{np+2}{\sqrt{np(1-p)}} + \frac{(n+4)\sqrt{p}}{\sqrt{n(1-p)}}$ is asymptotically standard normal. The lower and upper bounds of three-sigma control limits for the IWT $p$-chart are taken as follows: $P(Z < -3) + P(Z > 3) = 0.0027$. That is,

$$\begin{aligned} &P\left(\frac{(n+4)\left[f\left(\hat{p}_{\text{Adj}}\right)-f(p)-\frac{f''(p)e^2}{2}\right]}{|f'(p)|\sqrt{np(1-p)}}\right. \\ &\left.-\frac{np+2}{\sqrt{np(1-p)}}+\frac{(n+4)\sqrt{p}}{\sqrt{n(1-p)}}<-3\right) \\ &+P\left(\frac{(n+4)\left[f\left(\hat{p}_{\text{Adj}}\right)-f(p)-\frac{f''(p)e^2}{2}\right]}{|f'(p)|\sqrt{np(1-p)}}\right. \\ &\left.-\frac{np+2}{\sqrt{np(1-p)}}+\frac{(n+4)\sqrt{p}}{\sqrt{n(1-p)}}>3\right)=0.0027 \end{aligned} \tag{10}$$

Rearrange the terms in the two expressions of probabilities in Eq. (10) to get

$$\begin{aligned} &P\left(f\left(\hat{p}_{\text{Adj}}\right)<f(p)-\frac{3\,|f'(p)|\sqrt{np(1-p)}}{n+4}\right. \\ &\left.+\frac{|f'(p)|\,(np+2)}{n+4}-|f'(p)|\,p+\frac{f''(p)e^2}{2}\right) \\ &+P\left(f\left(\hat{p}_{\text{Adj}}\right)>f(p)+\frac{3\,|f'(p)|\sqrt{np(1-p)}}{n+4}\right. \\ &\left.+\frac{|f'(p)|\,(np+2)}{n+4}-|f'(p)|\,p+\frac{f''(p)e^2}{2}\right)=0.0027 \end{aligned}$$

Then, the IWT $p$-chart can be constructed with the center line as $CL_{\text{IWT}p} = f(p) = \sqrt{p}$. The first and second derivative of this function are $f'(p) = \frac{1}{2\sqrt{p}}$ and $f''(p) = -\frac{1}{4p\sqrt{p}}$, respectively. Then, the lower and upper bounds of three-sigma control limits for the IWT $p$-chart are given by Eqs. (11) and (12), respectively,

$$\begin{aligned} LCL_{\text{IWT}p} = f(p) &- \frac{3\,|f'(p)|\sqrt{np(1-p)}}{n+4} \\ &+\frac{|f'(p)|\,(np+2)}{n+4}-|f'(p)|\,p+\frac{f''(p)e^2}{2} \end{aligned} \tag{11}$$

$$\begin{aligned} UCL_{\text{IWT}p} = f(p) &+ \frac{3\,|f'(p)|\sqrt{np(1-p)}}{n+4} \\ &+\frac{|f'(p)|\,(np+2)}{n+4}-|f'(p)|\,p+\frac{f''(p)e^2}{2} \end{aligned} \tag{12}$$

For a small nonconforming fraction $p$, the binomial distribution is positively skewed. Therefore, it is not appropriate to use the control limits with equal tails. After the numerical exploration on some cases of the small nonconforming fraction of $p < 0.1$ and $n \leq 1,000$, the absolute errors (e) for the estimation of $p$ with $\hat{p}_{Adj} = \frac{X+2}{n+4}$ are suggested to be $\frac{5\sqrt{np(1-p)}}{n+4}$ for the $LCL_{\text{IWT}p}$ and $\frac{4\sqrt{np(1-p)}}{n+4}$ for the $UCL_{\text{IWT}p}$. Replacing the function of $f(p) = \sqrt{p}$ and its first and second derivatives with the recommended absolute errors in Eqs. (11) and (12), then the three-sigma of lower and upper control limits for the IWT $p$-chart are given by equations (13) and (14), respectively,

$$\begin{aligned} LCL_{\text{IWT}p} = \frac{\sqrt{p}}{2} &- \frac{3\sqrt{n(1-p)}}{2(n+4)} + \frac{np+2}{2(n+4)\sqrt{p}} \\ &- \frac{25n(1-p)}{8\sqrt{p}(n+4)^2} \end{aligned} \tag{13}$$

$$\begin{aligned} UCL_{\text{IWT}p} = \frac{\sqrt{p}}{2} &+ \frac{3\sqrt{n(1-p)}}{2(n+4)} + \frac{np+2}{2(n+4)\sqrt{p}} \\ &- \frac{2n(1-p)}{\sqrt{p}(n+4)^2} \end{aligned} \tag{14}$$

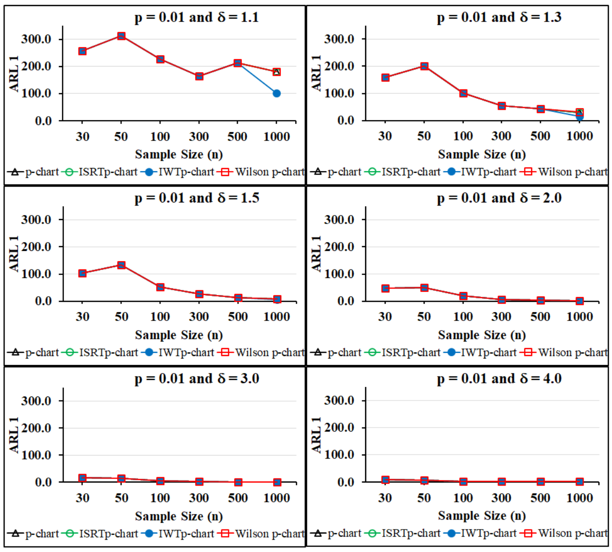


**Fig. 1.** Estimates of $ARL_1$ for four control charts in the case of $p_0 = 0.01$ and different shifts of nonconforming fraction

## 3. Results of the simulation study

The performances of the four control charts were compared via a simulation study. The nonconforming count data $(X_i)$ were generated in the form of a binomial distribution with two parameters that are set as follows: five levels of nonconforming fraction for in-control process $(p_0)$ are set as $0.01, 0.02, 0.05, 0.07$, and $0.09$ ; six levels of sample size $(n)$ are set as $30, 50, 100, 300, 500$, and $1000$. In addition, the subgroup size (m) was defined as 25 . For an out-of-control process, the shift in nonconforming fraction in the production process $(\delta)$ were set as $1.1, 1.3, 1.5, 2.0, 3.0$, and $4.0$ for $p_1 = p_0\delta$, where $p_1$ was the nonconforming fraction of an out-of-control process. The $ARL_0$ of all control

**Table 1.** Estimates of $ARL_1$ and $SDRL$ for four control charts in the case of $p_0 = 0.01$

| $n$ | $\delta$ | p-chart | | ISRT $p$-chart | | Wilson $p$-chart | | IWT p-chart | |
|---|---|---|---|---|---|---|---|---|---|
| | | ARL1 | SDRL | ARL1 | SDRL | ARL1 | SDRL | ARL1 | SDRL |
| 30 | 1.1 | 256.410 | 255.910 | 256.410 | 255.910 | 256.410 | 255.910 | 256.410 | 255.910 |
| | 1.3 | 158.730 | 158.229 | 158.730 | 158.229 | 158.730 | 158.229 | 158.730 | 158.229 |
| | 1.5 | 103.093 | 102.592 | 103.093 | 102.592 | 103.093 | 102.592 | 103.093 | 102.592 |
| | 2 | 47.847 | 47.344 | 47.847 | 47.344 | 47.847 | 47.344 | 47.847 | 47.344 |
| | 3 | 16.667 | 16.159 | 16.667 | 16.159 | 16.667 | 16.159 | 16.667 | 16.159 |
| | 4 | 8.569 | 8.053 | 8.569 | 8.053 | 8.569 | 8.053 | 8.569 | 8.053 |
| 50 | 1.1 | 312.500 | 312.000 | 312.500 | 312.000 | 312.500 | 312.000 | 312.500 | 312.000 |
| | 1.3 | 200.000 | 199.499 | 200.000 | 199.499 | 200.000 | 199.499 | 200.000 | 199.499 |
| | 1.5 | 133.333 | 132.832 | 133.333 | 132.832 | 133.333 | 132.832 | 133.333 | 132.832 |
| | 2 | 50.000 | 49.497 | 50.000 | 49.497 | 50.000 | 49.497 | 50.000 | 49.497 |
| | 3 | 15.456 | 14.948 | 15.456 | 14.948 | 15.456 | 14.948 | 15.456 | 14.948 |
| | 4 | 7.128 | 6.609 | 7.128 | 6.609 | 7.128 | 6.609 | 7.128 | 6.609 |
| 100 | 1.1 | 227.273 | 226.772 | 227.273 | 226.772 | 227.273 | 226.772 | 227.273 | 226.772 |
| | 1.3 | 102.041 | 101.540 | 102.041 | 101.540 | 102.041 | 101.540 | 102.041 | 101.540 |
| | 1.5 | 52.356 | 51.854 | 52.356 | 51.854 | 52.356 | 51.854 | 52.356 | 51.854 |
| | 2 | 19.305 | 18.798 | 19.305 | 18.798 | 19.305 | 18.798 | 19.305 | 18.798 |
| | 3 | 5.609 | 5.084 | 5.609 | 5.084 | 5.609 | 5.084 | 5.609 | 5.084 |
| | 4 | 2.714 | 2.156 | 2.714 | 2.156 | 2.714 | 2.156 | 2.714 | 2.156 |
| 300 | 1.1 | 163.934 | 163.434 | 163.934 | 163.434 | 163.934 | 163.434 | 163.934 | 163.434 |
| | 1.3 | 55.556 | 55.053 | 55.556 | 55.053 | 55.556 | 55.053 | 55.556 | 55.053 |
| | 1.5 | 25.974 | 25.469 | 25.974 | 25.469 | 25.974 | 25.469 | 25.974 | 25.469 |
| | 2 | 6.716 | 6.196 | 6.716 | 6.196 | 6.716 | 6.196 | 6.716 | 6.196 |
| | 3 | 1.841 | 1.245 | 1.841 | 1.245 | 1.841 | 1.245 | 1.841 | 1.245 |
| | 4 | 1.176 | 0.455 | 1.176 | 0.455 | 1.176 | 0.455 | 1.176 | 0.455 |
| 500 | 1.1 | 212.766 | 212.265 | 212.766 | 212.265 | 212.766 | 212.265 | 212.766 | 212.265 |
| | 1.3 | 43.668 | 43.165 | 43.668 | 43.165 | 43.668 | 43.165 | 43.668 | 43.165 |
| | 1.5 | 14.045 | 13.536 | 14.045 | 13.536 | 14.045 | 13.536 | 14.045 | 13.536 |
| | 2 | 3.113 | 2.565 | 3.113 | 2.565 | 3.113 | 2.565 | 3.113 | 2.565 |
| | 3 | 1.212 | 0.507 | 1.212 | 0.507 | 1.212 | 0.507 | 1.212 | 0.507 |
| | 4 | 1.027 | 0.167 | 1.027 | 0.167 | 1.027 | 0.167 | 1.027 | 0.167 |
| 1000 | 1.1 | 181.818 | 181.318 | 181.818 | 181.318 | 181.818 | 181.318 | **102.041** | **101.540** |
| | 1.3 | 28.818 | 28.314 | 28.818 | 28.314 | 30.769 | 30.265 | **16.447** | **15.940** |
| | 1.5 | 8.143 | 7.627 | 8.143 | 7.627 | 8.382 | 7.866 | **5.414** | **4.889** |
| | 2 | 1.812 | 1.213 | 1.812 | 1.213 | 1.831 | 1.234 | **1.559** | **0.934** |
| | 3 | 1.025 | 0.159 | 1.025 | 0.159 | 1.027 | 0.165 | **1.016** | **0.129** |
| | 4 | 1.001 | 0.022 | 1.001 | 0.022 | **1.000** | 0.017 | **1.000** | **0.010** |

charts was set at 370.4 because the proposed chart (IWT $p$-chart) was derived based only on three-sigma control limits. The details of the proof are in Theorem 3. Therefore, in the data simulation, the efficiency comparison of three-sigma control limits was investigated. In many past studies, it was found that most chart performance comparisons gave the same analytical results regardless of the level of the $ARL_0$ used [12]. Therefore, the performance comparison of the four control charts tested in this study focused on $ARL_1$ and $SDRL$ of three sigma control to determine which chart will have the most sensitive ability to detect process changes. This simulation study was conducted with a Monte Carlo technique for 180 situations and repeated 10,000 times for each situation. The performance comparison measures were the estimates of $ARL_1$ and $SDRL$. The control chart with the lowest $ARL_1$ and $SDRL$ was the most effective chart for detection of the shift in the process. The simulation results are shown in Tables 1 to 5. Table 1 shows that the efficiencies of all control charts tend to be the same for $p_0 = 0.01$ and sample sizes of $30, 50, 100, 300$ and 500 . However, the IWT $p$-chart was distinctly the most efficient for detecting all the shifts in nonconforming fraction with a large sample size of 1000. In addition, the $ARL_1s$ and SDRLs of all control charts tended to decrease when the sample sizes and the shift in nonconforming fraction increased. Especially for a very large shift in nonconforming fraction of 4.0 and large sample size of 1000, the $ARL_1s$ and $SDRL$s of all control charts were

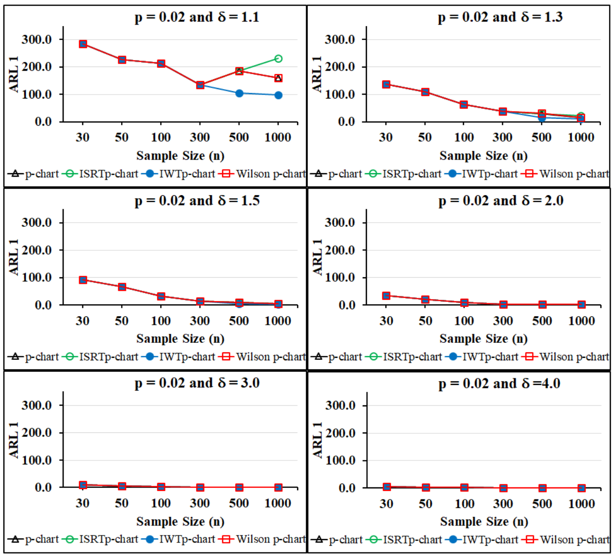


**Fig. 2.** Estimates of $ARL_1$ for four control charts in the case of $p_0 = 0.02$ and different shifts of nonconforming fraction

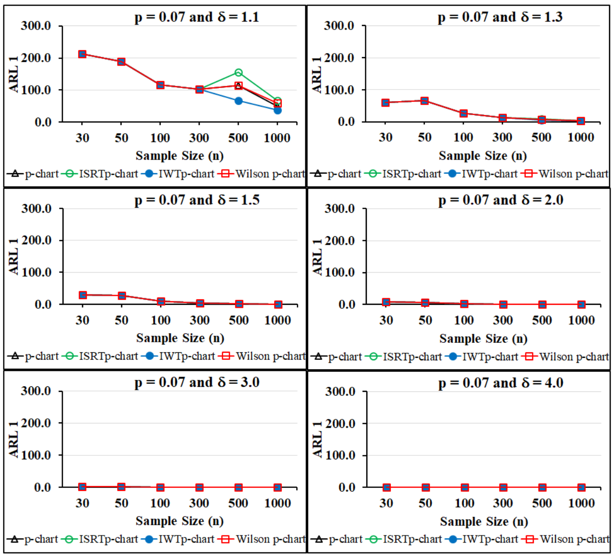


**Fig. 4.** Estimates of $ARL_1$ for four control charts in the case of $p_0 = 0.07$ and different shifts of nonconforming fraction

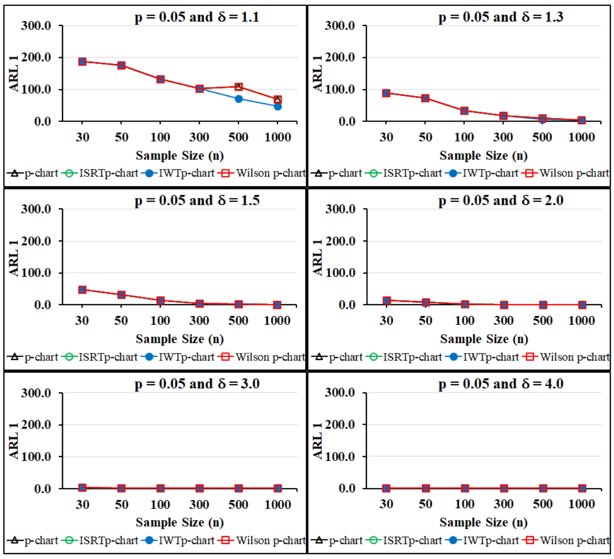


**Fig. 3.** Estimates of $ARL_1$ for four control charts in the case of $p_0 = 0.05$ and different shifts of nonconforming fraction

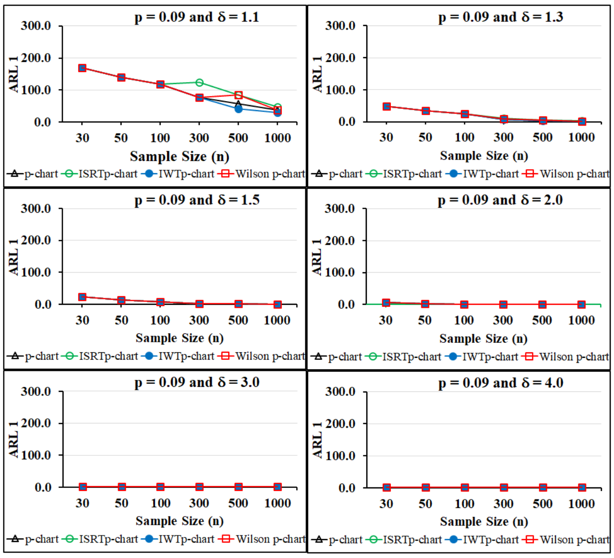


**Fig. 5.** Estimates of $ARL_1$ for four control charts in the case of $p_0 = 0.09$ and different shifts of nonconforming fraction

close to 1 and 0, respectively. Tables 2 to 5 show that the efficiencies of all control charts were the same for $p_0$ equals to 0.02, 0.05, 0.07, and 0.09 and sample sizes of 30, 50, 100, and 300. Moreover, the IWT $p$-chart was the most efficient for sample sizes of 500 and 1000, especially for a small shift in nonconforming fraction. For a large sample size of 1000 and a small shift in nonconforming fraction, the ability of ISRT $p$-chart to detect an out-of-control process was relatively poor compared to the other three charts. Further, the $ARL_1s$ and $SDRLs$ of all control charts tended to decrease when the sample size and the shift in nonconforming fraction increased. That is, the $ARL_1s$ and $SDRLs$ of all control charts tend to be 1 and 0 , respectively for a large shift in nonconforming fraction and sample sizes of 300, 500, and 1000.

Figs. 1 to 5 show that the $ARL_1s$ of all control charts, when the sample size increased, tended to decrease rapidly for a small level of the shift in nonconforming fraction, for $p_0 = 0.01, 0.02, 0.05, 0.07,$ and 0.09. In addition, the proposed IWT $p$-chart was the most efficient for large sample sizes of 500 and 1000, especially for a small shift in the nonconforming fraction, such as $\delta = 1.1$, in this simulation

**Table 2.** Estimates of $ARL_1$ and $SDRL$ for four control charts in the case of $p_0 = 0.02$

| $n$ | $\delta$ | p-chart | | ISRT $p$-chart | | Wilson $p$-chart | | IWT $p$-chart | |
|---|---|---|---|---|---|---|---|---|---|
| | | ARL1 | SDRL | ARL1 | SDRL | ARL1 | SDRL | ARL1 | SDRL |
| 30 | 1.1 | 285.714 | 285.214 | 285.714 | 285.214 | 285.714 | 285.214 | 285.714 | 285.214 |
| | 1.3 | 136.986 | 136.485 | 136.986 | 136.485 | 136.986 | 136.485 | 136.986 | 136.485 |
| | 1.5 | 90.909 | 90.408 | 90.909 | 90.408 | 90.909 | 90.408 | 90.909 | 90.408 |
| | 2 | 34.722 | 34.219 | 34.722 | 34.219 | 34.722 | 34.219 | 34.722 | 34.219 |
| | 3 | 9.823 | 9.310 | 9.823 | 9.310 | 9.823 | 9.310 | 9.823 | 9.310 |
| | 4 | 4.710 | 4.181 | 4.710 | 4.181 | 4.710 | 4.181 | 4.710 | 4.181 |
| 50 | 1.1 | 227.273 | 226.772 | 227.273 | 226.772 | 227.273 | 226.772 | 227.273 | 226.772 |
| | 1.3 | 109.890 | 109.389 | 109.890 | 109.389 | 109.890 | 109.389 | 109.890 | 109.389 |
| | 1.5 | 66.667 | 66.165 | 66.667 | 66.165 | 66.667 | 66.165 | 66.667 | 66.165 |
| | 2 | 21.231 | 20.725 | 21.231 | 20.725 | 21.231 | 20.725 | 21.231 | 20.725 |
| | 3 | 5.731 | 5.207 | 5.731 | 5.207 | 5.731 | 5.207 | 5.731 | 5.207 |
| | 4 | 2.690 | 2.132 | 2.690 | 2.132 | 2.690 | 2.132 | 2.690 | 2.132 |
| 100 | 1.1 | 212.766 | 212.265 | 212.766 | 212.265 | 212.766 | 212.265 | 212.766 | 212.265 |
| | 1.3 | 63.291 | 62.789 | 63.291 | 62.789 | 63.291 | 62.789 | 63.291 | 62.789 |
| | 1.5 | 31.646 | 31.142 | 31.646 | 31.142 | 31.646 | 31.142 | 31.646 | 31.142 |
| | 2 | 9.470 | 8.956 | 9.470 | 8.956 | 9.470 | 8.956 | 9.470 | 8.956 |
| | 3 | 2.559 | 1.997 | 2.559 | 1.997 | 2.559 | 1.997 | 2.559 | 1.997 |
| | 4 | 1.428 | 0.781 | 1.428 | 0.781 | 1.428 | 0.781 | 1.428 | 0.781 |
| 300 | 1.1 | 135.135 | 134.634 | 135.135 | 134.634 | 135.135 | 134.634 | 135.135 | 134.634 |
| | 1.3 | 39.370 | 38.867 | 39.370 | 38.867 | 39.370 | 38.867 | 39.370 | 38.867 |
| | 1.5 | 14.535 | 14.026 | 14.535 | 14.026 | 14.535 | 14.026 | 14.535 | 14.026 |
| | 2 | 3.169 | 2.621 | 3.169 | 2.621 | 3.169 | 2.621 | 3.169 | 2.621 |
| | 3 | 1.160 | 0.430 | 1.160 | 0.430 | 1.160 | 0.430 | 1.160 | 0.430 |
| | 4 | 1.009 | 0.094 | 1.009 | 0.094 | 1.009 | 0.094 | 1.009 | 0.094 |
| 500 | 1.1 | 185.185 | 184.685 | 185.185 | 184.685 | 185.185 | 184.685 | **106.383** | **105.882** |
| | 1.3 | 29.326 | 28.821 | 29.326 | 28.821 | 31.447 | 30.942 | **16.000** | **15.492** |
| | 1.5 | 8.217 | 7.701 | 8.217 | 7.701 | 8.511 | 7.995 | **5.565** | **5.040** |
| | 2 | 1.835 | 1.238 | 1.835 | 1.238 | 1.830 | 1.232 | **1.575** | **0.951** |
| | 3 | 1.025 | 0.159 | 1.025 | 0.159 | 1.025 | 0.161 | **1.015** | **0.123** |
| | 4 | **1.000** | 0.017 | **1.000** | 0.017 | **1.000** | **0.010** | **1.000** | **0.010** |
| 1000 | 1.1 | 161.290 | 160.790 | 232.558 | 232.058 | 161.290 | 160.790 | **98.039** | **97.538** |
| | 1.3 | 14.837 | 14.328 | 22.779 | 22.273 | 14.837 | 14.328 | **10.309** | **9.797** |
| | 1.5 | 3.876 | 3.339 | 4.960 | 4.432 | 3.876 | 3.339 | **3.086** | **2.538** |
| | 2 | 1.171 | 0.447 | 1.229 | 0.530 | 1.171 | 0.447 | **1.125** | **0.375** |
| | 3 | **1.000** | **0.000** | **1.000** | 0.010 | **1.000** | **0.000** | **1.000** | **0.000** |
| | 4 | **1.000** | **0.000** | **1.000** | **0.000** | **1.000** | **0.000** | **1.000** | **0.000** |

study.

## 4. Real-life application

A real-life data set for the three-sigma control limits construction of four charts-IWT p-chart, $p$-chart, ISRT $p$-chart and Wilson $p$-chart-was taken from Montgomery [4]. It was related to a production process of orange juice which was packed in 6 -ounce cardboard cans. These cans are inspected for possible non-compliance, such as leaks in the side seams or at the bottom joint. Cans that do not meet these requirements may have improper sealing at the side seams or bottom panel. These four control charts can be used to improve the fraction of nonconforming cans produced by this process. To establish these, samples of 50 cans were randomly drawn to check the quality over a period of half an hour over the course of three shifts in which the machine was continuously running. Data were collected from a total of 30 subgroups. The information is shown in Table 6.

The initial control limits of four control charts for the data in Table 6 are shown in Fig. 6. The plot statistics for each chart from the initial subgroup are plotted on these charts. Fig. 6 shows that there are two points from subgroups 15 and 23 that are above the upper control limits for all control charts. These points had to be investigated to see whether an assignable cause can be determined. The inspection revealed that a new batch of cardboard stock had been produced during that half-hour period in sub-

**Table 3.** Estimates of $ARL_1$ and SDRL for four control charts in the case of $p_0 = 0.05$

| $n$ | $\delta$ | $p$-chart |  | ISRT $p$-chart |  | Wilson p-chart |  | IWT p-chart |  |
|---|---|---|---|---|---|---|---|---|---|
|  |  | ARL1 | SDRL | ARL1 | SDRL | ARL1 | SDRL | ARL1 | SDRL |
| 30 | 1.1 | 188.679 | 188.179 | 188.679 | 188.179 | 188.679 | 188.179 | 188.679 | 188.179 |
|  | 1.3 | 88.496 | 87.994 | 88.496 | 87.994 | 88.496 | 87.994 | 88.496 | 87.994 |
|  | 1.5 | 47.619 | 47.116 | 47.619 | 47.116 | 47.619 | 47.116 | 47.619 | 47.116 |
|  | 2 | 13.870 | 13.360 | 13.870 | 13.360 | 13.870 | 13.360 | 13.870 | 13.360 |
|  | 3 | 3.461 | 2.919 | 3.461 | 2.919 | 3.461 | 2.919 | 3.461 | 2.919 |
|  | 4 | 1.751 | 1.146 | 1.751 | 1.146 | 1.751 | 1.146 | 1.751 | 1.146 |
| 50 | 1.1 | 175.439 | 174.938 | 175.439 | 174.938 | 175.439 | 174.938 | 175.439 | 174.938 |
|  | 1.3 | 74.074 | 73.572 | 74.074 | 73.572 | 74.074 | 73.572 | 74.074 | 73.572 |
|  | 1.5 | 33.445 | 32.941 | 33.445 | 32.941 | 33.445 | 32.941 | 33.445 | 32.941 |
|  | 2 | 8.231 | 7.714 | 8.231 | 7.714 | 8.231 | 7.714 | 8.231 | 7.714 |
|  | 3 | 2.064 | 1.482 | 2.064 | 1.482 | 2.064 | 1.482 | 2.064 | 1.482 |
|  | 4 | 1.236 | 0.540 | 1.236 | 0.540 | 1.236 | 0.540 | 1.236 | 0.540 |
| 100 | 1.1 | 133.333 | 132.832 | 133.333 | 132.832 | 133.333 | 132.832 | 133.333 | 132.832 |
|  | 1.3 | 33.333 | 32.829 | 33.333 | 32.829 | 33.333 | 32.829 | 33.333 | 32.829 |
|  | 1.5 | 14.144 | 13.635 | 14.144 | 13.635 | 14.144 | 13.635 | 14.144 | 13.635 |
|  | 2 | 3.413 | 2.870 | 3.413 | 2.870 | 3.413 | 2.870 | 3.413 | 2.870 |
|  | 3 | 1.194 | 0.481 | 1.194 | 0.481 | 1.194 | 0.481 | 1.194 | 0.481 |
|  | 4 | 1.013 | 0.115 | 1.013 | 0.115 | 1.013 | 0.115 | 1.013 | 0.115 |
| 300 | 1.1 | 103.093 | 102.592 | 103.093 | 102.592 | 103.093 | 102.592 | 103.093 | 102.592 |
|  | 1.3 | 18.248 | 17.741 | 18.248 | 17.741 | 18.248 | 17.741 | 18.248 | 17.741 |
|  | 1.5 | 5.465 | 4.939 | 5.465 | 4.939 | 5.465 | 4.939 | 5.465 | 4.939 |
|  | 2 | 1.343 | 0.679 | 1.343 | 0.679 | 1.343 | 0.679 | 1.343 | 0.679 |
|  | 3 | 1.001 | 0.025 | 1.001 | 0.025 | 1.001 | 0.025 | 1.001 | 0.025 |
|  | 4 | 1.000 | 0.000 | 1.000 | 0.000 | 1.000 | 0.000 | 1.000 | 0.000 |
| 500 | 1.1 | 109.890 | 109.389 | 109.890 | 109.389 | 109.890 | 109.389 | **71.429** | **70.927** |
|  | 1.3 | 9.718 | 9.205 | 9.718 | 9.205 | 9.718 | 9.205 | **7.067** | **6.548** |
|  | 1.5 | 2.717 | 2.160 | 2.717 | 2.160 | 2.717 | 2.160 | **2.313** | **1.743** |
|  | 2 | 1.059 | 0.251 | 1.059 | 0.251 | 1.059 | 0.251 | **1.045** | **0.216** |
|  | 3 | **1.000** | **0.000** | **1.000** | **0.000** | **1.000** | **0.000** | **1.000** | **0.000** |
|  | 4 | **1.000** | **0.000** | **1.000** | **0.000** | **1.000** | **0.000** | **1.000** | **0.000** |
| 1000 | 1.1 | 68.966 | 68.464 | 68.966 | 68.464 | 68.966 | 68.464 | **47.847** | **47.344** |
|  | 1.3 | 4.148 | 3.613 | 4.148 | 3.613 | 4.148 | 3.613 | **3.511** | **2.969** |
|  | 1.5 | 1.416 | 0.768 | 1.416 | 0.768 | 1.416 | 0.768 | **1.339** | **0.674** |
|  | 2 | 1.001 | 0.026 | 1.001 | 0.026 | 1.001 | 0.026 | **1.000** | **0.020** |
|  | 3 | **1.000** | **0.000** | **1.000** | **0.000** | **1.000** | **0.000** | **1.000** | **0.000** |
|  | 4 | **1.000** | **0.000** | **1.000** | **0.000** | **1.000** | **0.000** | **1.000** | **0.000** |

group of 15 , and there is a reasonable ground to believe that assignable cause had also occurred here. Additionally, subgroup 23's inexperienced operator was temporarily assigned to the machine and this may cause a high fraction of non-conforming cans from that subgroup. Therefore, samples from subgroups 15 and 23 were eliminated and the new control limits of the four control charts are shown in Table 7.

The plot statistics for the revised control limits of $p$-chart and Wilson $p$-chart are given by the nonconforming fraction of a sample or $\hat{p}_i = \frac{X_i}{n}$, but those for ISRT $p$-chart and IWT $p$-chart are $f(\hat{p}_i) = \sqrt{\frac{X_i}{n}}$ and $f\left(\hat{p}_{Adj_i}\right) = \sqrt{\frac{X_i+2}{n+4}}$, respectively. Although the proportion of nonconforming cans in subgroup 21 was still outside the upper control limits of three charts, namely $p$-chart, Wilson $p$-chart and IWT $p$-chart, there was no effect of an assignable cause. Therefore, the data in subgroup 21 were retained and those revised control limits in Table 7 were applied for further production control process.

## 5. Discussions

In this research, the efficiency of IWT $p$-chart was compared with these of $p$-chart, ISRT $p$-chart, and Wilson $p$-chart via a simulation study. It was found that the sensitivity to detect an out-of-control process of IWT $p$-chart tended to be better than the other two charts for a small nonconforming fraction in the process because the proposed chart was derived from a transformation concept of Tsai et al. [15]

**Table 4.** Estimates of $ARL_1$ and $SDRL$ for four control charts in the case of $p_0 = 0.07$

| $n$ | $\delta$ | p-chart | | ISRT $p$-chart | | Wilson $p$-chart | | IWT $p$-chart | |
|---|---|---|---|---|---|---|---|---|---|
| | | ARL1 | SDRL | ARL1 | SDRL | ARL1 | SDRL | ARL1 | SDRL |
| 30 | 1.1 | 212.766 | 212.265 | 212.766 | 212.265 | 212.766 | 212.265 | 212.766 | 212.265 |
| | 1.3 | 60.606 | 60.104 | 60.606 | 60.104 | 60.606 | 60.104 | 60.606 | 60.104 |
| | 1.5 | 29.762 | 29.258 | 29.762 | 29.258 | 29.762 | 29.258 | 29.762 | 29.258 |
| | 2 | 8.718 | 8.203 | 8.718 | 8.203 | 8.718 | 8.203 | 8.718 | 8.203 |
| | 3 | 2.243 | 1.669 | 2.243 | 1.669 | 2.243 | 1.669 | 2.243 | 1.669 |
| | 4 | 1.283 | 0.602 | 1.283 | 0.602 | 1.283 | 0.602 | 1.283 | 0.602 |
| 50 | 1.1 | 188.679 | 188.179 | 188.679 | 188.179 | 188.679 | 188.179 | 188.679 | 188.179 |
| | 1.3 | 67.114 | 66.612 | 67.114 | 66.612 | 67.114 | 66.612 | 67.114 | 66.612 |
| | 1.5 | 28.169 | 27.664 | 28.169 | 27.664 | 28.169 | 27.664 | 28.169 | 27.664 |
| | 2 | 6.460 | 5.939 | 6.460 | 5.939 | 6.460 | 5.939 | 6.460 | 5.939 |
| | 3 | 1.583 | 0.960 | 1.583 | 0.960 | 1.583 | 0.960 | 1.583 | 0.960 |
| | 4 | 1.076 | 0.285 | 1.076 | 0.285 | 1.076 | 0.285 | 1.076 | 0.285 |
| 100 | 1.1 | 116.279 | 115.778 | 116.279 | 115.778 | 116.279 | 115.778 | 116.279 | 115.778 |
| | 1.3 | 27.322 | 26.818 | 27.322 | 26.818 | 27.322 | 26.818 | 27.322 | 26.818 |
| | 1.5 | 10.122 | 9.608 | 10.122 | 9.608 | 10.122 | 9.608 | 10.122 | 9.608 |
| | 2 | 2.339 | 1.769 | 2.339 | 1.769 | 2.339 | 1.769 | 2.339 | 1.769 |
| | 3 | 1.050 | 0.229 | 1.050 | 0.229 | 1.050 | 0.229 | 1.050 | 0.229 |
| | 4 | 1.001 | 0.025 | 1.001 | 0.025 | 1.001 | 0.025 | 1.001 | 0.025 |
| 300 | 1.1 | 103.093 | 102.592 | 103.093 | 102.592 | 103.093 | 102.592 | 103.093 | 102.592 |
| | 1.3 | 13.280 | 12.770 | 13.280 | 12.770 | 13.193 | 12.683 | 13.280 | 12.770 |
| | 1.5 | 3.592 | 3.051 | 3.592 | 3.051 | 3.635 | 3.095 | 3.592 | 3.051 |
| | 2 | 1.116 | 0.359 | 1.116 | 0.359 | 1.117 | 0.361 | 1.116 | 0.359 |
| | 3 | 1.000 | 0.000 | 1.000 | 0.000 | 1.000 | 0.000 | 1.000 | 0.000 |
| | 4 | 1.000 | 0.000 | 1.000 | 0.000 | 1.000 | 0.000 | 1.000 | 0.000 |
| | 1.1 | 114.943 | 114.441 | 156.250 | 155.749 | 114.943 | 114.441 | **66.225** | **65.723** |
| 500 | 1.3 | 7.174 | 6.655 | 9.470 | 8.956 | 7.062 | 6.543 | **5.631** | **5.106** |
| | 1.5 | 2.006 | 1.420 | 2.253 | 1.680 | 1.966 | 1.378 | **1.786** | **1.185** |
| | 2 | 1.013 | 0.116 | 1.018 | 0.135 | 1.013 | 0.113 | **1.010** | **0.098** |
| | 3 | **1.000** | **0.000** | **1.000** | **0.000** | **1.000** | **0.000** | **1.000** | **0.000** |
| | 4 | **1.000** | **0.000** | **1.000** | **0.000** | **1.000** | **0.000** | **1.000** | **0.000** |
| 1000 | 1.1 | 49.261 | 48.759 | 66.667 | 66.165 | 58.480 | 57.977 | **37.594** | **37.091** |
| | 1.3 | 2.848 | 2.294 | 3.204 | 2.657 | 2.848 | 2.294 | **2.538** | **1.976** |
| | 1.5 | 1.158 | 0.428 | 1.194 | 0.481 | 1.162 | 0.433 | **1.127** | **0.377** |
| | 2 | 1.000 | 0.010 | 1.000 | 0.010 | **1.000** | **0.000** | **1.000** | **0.010** |
| | 3 | **1.000** | **0.000** | **1.000** | **0.000** | **1.000** | **0.000** | **1.000** | **0.000** |
| | 4 | **1.000** | **0.000** | **1.000** | **0.000** | **1.000** | **0.000** | **1.000** | **0.000** |

and adjusted Wald confidence interval estimation concept. These two concepts tend to be performed well efficiency of inference for a low level of nonconforming fraction as a result of zero nonconforming items in the favorite process [13, 20]. The out-of-control average run length and standard deviation of the run length tended to decrease when the sample size and the shift of nonconforming fraction increased, agreeing with the results of Sinsomboonthong and Sinsomboonthong [5], Rod-o et al. [13], Tsai et al. [15], and Aslam et al. [31]. The ISRT $p$-chart tended to have a good efficiency for a large shift in nonconforming fraction and large sample size, agreeing with Sukparungsee [12] and Tsai et al. [15]. The strength of the proposed chart is its effectiveness in fast-detecting abnormalities in the process even if the nonconforming fraction slightly changes from the target during that time. Moreover, the proposed chart does not have complicated formulas and so easy to apply in real life. In addition, the proposed chart only considers the data collected during a short period of production time, a true reflection of the actual production process.

## 6. Conclusions

In this research, the efficiencies or the out-of-control process detection sensitivity of four charts-p-chart, ISRT $p$-chart, Wilson $p$-chart and IWT $p$-chart-were compared. The comparison was especially for the case of low nonconforming rate commonly occurred in a manufacturing process. The appropriate nonconforming fraction control charts for each

**Table 5.** Estimates of $ARL_1$ and SDRL for four control charts in the case of $p_0 = 0.09$

| $n$ | $\delta$ | p-chart | | ISRT $p$-chart | | Wilson $p$-chart | | IWT $p$-chart | |
|---|---|---|---|---|---|---|---|---|---|
| | | ARL1 | SDRL | ARL1 | SDRL | ARL1 | SDRL | ARL1 | SDRL |
| 30 | 1.1 | 169.492 | 168.991 | 169.492 | 168.991 | 169.492 | 168.991 | 169.492 | 168.991 |
| | 1.3 | 49.505 | 49.002 | 49.505 | 49.002 | 49.505 | 49.002 | 49.505 | 49.002 |
| | 1.5 | 24.450 | 23.945 | 24.450 | 23.945 | 24.450 | 23.945 | 24.450 | 23.945 |
| | 2 | 6.382 | 5.860 | 6.382 | 5.860 | 6.382 | 5.860 | 6.382 | 5.860 |
| | 3 | 1.699 | 1.089 | 1.699 | 1.089 | 1.699 | 1.089 | 1.699 | 1.089 |
| | 4 | 1.112 | 0.352 | 1.112 | 0.352 | 1.112 | 0.352 | 1.112 | 0.352 |
| 50 | 1.1 | 140.845 | 140.344 | 140.845 | 140.344 | 140.845 | 140.344 | 140.845 | 140.344 |
| | 1.3 | 35.587 | 35.084 | 35.587 | 35.084 | 35.587 | 35.084 | 35.587 | 35.084 |
| | 1.5 | 14.993 | 14.484 | 14.993 | 14.484 | 14.993 | 14.484 | 14.993 | 14.484 |
| | 2 | 3.610 | 3.070 | 3.610 | 3.070 | 3.610 | 3.070 | 3.610 | 3.070 |
| | 3 | 1.204 | 0.495 | 1.204 | 0.495 | 1.204 | 0.495 | 1.204 | 0.495 |
| | 4 | 1.012 | 0.112 | 1.012 | 0.112 | 1.012 | 0.112 | 1.012 | 0.112 |
| 100 | 1.1 | 117.647 | 117.146 | 117.647 | 117.146 | 117.647 | 117.146 | 117.647 | 117.146 |
| | 1.3 | 25.126 | 24.621 | 25.126 | 24.621 | 25.126 | 24.621 | 25.126 | 24.621 |
| | 1.5 | 8.190 | 7.674 | 8.190 | 7.674 | 8.190 | 7.674 | 8.190 | 7.674 |
| | 2 | 1.840 | 1.243 | 1.840 | 1.243 | 1.840 | 1.243 | 1.840 | 1.243 |
| | 3 | 1.013 | 0.113 | 1.013 | 0.113 | 1.013 | 0.113 | 1.013 | 0.113 |
| | 4 | 1.000 | 0.000 | 1.000 | 0.000 | 1.000 | 0.000 | 1.000 | 0.000 |
| 300 | 1.1 | 76.336 | 75.834 | 76.336 | 75.834 | 76.336 | 75.834 | 76.336 | 75.834 |
| | 1.3 | 7.975 | 7.458 | 7.975 | 7.458 | 8.231 | 7.714 | 7.975 | 7.458 |
| | 1.5 | 2.358 | 1.789 | 2.358 | 1.789 | 2.391 | 1.824 | 2.358 | 1.789 |
| | 2 | 1.025 | 0.160 | 1.025 | 0.160 | 1.027 | 0.167 | 1.025 | 0.160 |
| | 3 | 1.000 | 0.000 | 1.000 | 0.000 | 1.000 | 0.000 | 1.000 | 0.000 |
| | 4 | 1.000 | 0.000 | 1.000 | 0.000 | 1.000 | 0.000 | 1.000 | 0.000 |
| 500 | 1.1 | 56.180 | 55.678 | 85.470 | 84.969 | 85.470 | 84.969 | **41.322** | **40.819** |
| | 1.3 | 4.198 | 3.664 | 5.051 | 4.523 | 5.051 | 4.523 | **3.552** | **3.011** |
| | 1.5 | 1.432 | 0.786 | 1.526 | 0.895 | 1.526 | 0.895 | **1.346** | **0.683** |
| | 2 | 1.001 | 0.033 | 1.002 | 0.042 | 1.002 | 0.042 | **1.001** | **0.028** |
| | 3 | **1.000** | **0.000** | **1.000** | **0.000** | **1.000** | **0.000** | **1.000** | **0.000** |
| | 4 | **1.000** | **0.000** | **1.000** | **0.000** | **1.000** | **0.000** | **1.000** | **0.000** |
| 1000 | 1.1 | 37.594 | 37.091 | 46.948 | 46.446 | 37.594 | 37.091 | **29.851** | **29.346** |
| | 1.3 | 2.088 | 1.507 | 2.271 | 1.699 | 2.064 | 1.482 | **1.917** | **1.326** |
| | 1.5 | 1.054 | 0.239 | 1.066 | 0.264 | 1.053 | 0.235 | **1.045** | **0.216** |
| | 2 | **1.000** | **0.000** | **1.000** | **0.000** | **1.000** | **0.000** | **1.000** | **0.000** |
| | 3 | **1.000** | **0.000** | **1.000** | **0.000** | **1.000** | **0.000** | **1.000** | **0.000** |
| | 4 | **1.000** | **0.000** | **1.000** | **0.000** | **1.000** | **0.000** | **1.000** | **0.000** |

of 180 situations are shown in Table 8.

Table 8 shows that the proposed IWT $p$-chart tended to perform with the best efficiency for large sample sizes of 500 and 1000 and the level of nonconforming fraction below 0.1 whatever the shift in nonconforming fraction was. However, for a smaller sample size, $n < 500$, the IWT $p$-chart provided the same efficiency as the $p$-chart and ISRT $p$-chart and Wilson $p$-chart. The out-of-control average run length had a downward trend for an increase in sample size and shift of nonconforming fraction.

## 7. Acknowledgments

This research was financial supported by School of Science, King Mongkut's Institute of Technology Ladkrabang for funding of the research project on "New Improved $p$-Chart and $np$-Chart Transformations" (Grant no. 2566-02-05-004). Moreover, this research would not been successfully without support from International SciKU Branding (ISB), Faculty of Science, Kasetsart University. The authors would like to express special thanks to the executives of both institutions for their supports of this research.

## References

**[1]** M. Crawford and A. D. Benedetto. *New Products Management*. McGraw-Hill, 2015.

**[2]** D. H. Besterfield. *Quality Control*. Pearson Prentice Hall New Jersey, 2009.

**Table 6.** Data for nonconforming cans produced in the process

| Subgroup number | Number of nonconforming cans $(X_i)$ | Subgroup number | Number of nonconforming cans $(X_i)$ | Subgroup number | Number of nonconforming cans $(X_i)$ |
|---|---|---|---|---|---|
| 1 | 12 | 11 | 5 | 21 | 20 |
| 2 | 15 | 12 | 6 | 22 | 18 |
| 3 | 8 | 13 | 17 | 23 | 24 |
| 4 | 10 | 14 | 12 | 24 | 15 |
| 5 | 4 | 15 | 22 | 25 | 9 |
| 6 | 7 | 16 | 8 | 26 | 12 |
| 7 | 16 | 17 | 10 | 27 | 7 |
| 8 | 9 | 18 | 5 | 28 | 13 |
| 9 | 14 | 19 | 13 | 29 | 9 |
| 10 | 10 | 20 | 11 | 30 | 6 |

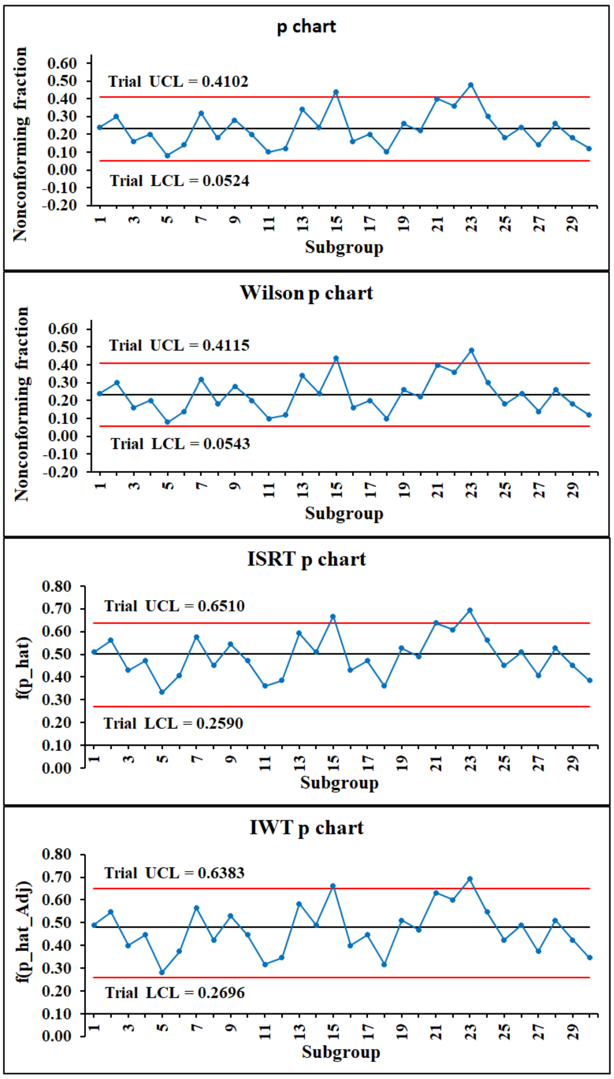


**Fig. 6.** Initial control limits of four control charts for data in Table 6

**Table 7.** Revised control limits of four control charts

| Control chart | Lower control limit | Upper control limit |
|---|---|---|
| $p$-chart | 0.0407 | 0.3893 |
| Wilson $p$-chart | 0.0428 | 0.3908 |
| ISRT $p$-chart | 0.2376 | 0.6347 |
| IWT $p$-chart | 0.2501 | 0.6238 |


[3] A. Mitra. *Fundamentals of Quality Control and Improvement*. John Wiley and Sons, 2021.

[4] D. C. Montgomery. *Introduction to Statistical Quality Control*. John Wiley and Sons, 2019.

[5] J. Sinsomboonthong and S. Sinsomboonthong, (2021) *"New quality control chart to quickly detect the changes of process average."* **Quality-Access to Success** *22*(184): 21–33. DOI: 10.47750/QAS/22.184.03.

[6] R. Goedhart and W. H. Woodall, (2022) *"Monitoring proportions with two components of common cause variation"* **Journal of Quality Technology** *54*(3): 324–337. DOI: 10.1080/00224065.2021.1903823.

[7] Z. Abbas, H. Z. Nazir, N. Akhtar, M. Abid, and M. Riaz, (2020) *"On designing an efficient control chart to monitor fraction nonconforming"* **Quality and Reliability Engineering International** *36*(2): 547–564. DOI: 10.1002/qre.2590.

[8] M. Ahsan, M. Mashuri, and H. Khusna, (2017) *"Evaluation of Laney p'chart performance"* **International Journal of Applied Engineering Research** *12*(24): 14208–14217.

[9] S. Chakraborti and S. W. Human, (2006) *"Parameter estimation and performance of the p-chart for attribute data"* **IEEE Transactions on Reliability** *55*(3): 559–566. DOI: 10.1109/TR.2006.879662.

[10] S. Joekes and E. P. Barbosa, (2013) *"An improved attribute control chart for monitoring non-conforming proportion in high quality processes"* **Control Engineering**

**Table 8.** Appropriate nonconforming fraction control chart(s) for each situation

| $n$ | $\delta$ | Nonconforming fraction of in-control process ($p_0$) 0.01 | 0.02 | 0.05 | 0.07 | 0.09 |
|---|---|---|---|---|---|---|
| 30 | 1.1 | All | All | All | All | All |
| | 1.3 | All | All | All | All | All |
| | 1.5 | All | All | All | All | All |
| | 2.0 | All | All | All | All | All |
| | 3.0 | All | All | All | All | All |
| | 4.0 | All | All | All | All | All |
| 50 | 1.1 | All | All | All | All | All |
| | 1.3 | All | All | All | All | All |
| | 1.5 | All | All | All | All | All |
| | 2.0 | All | All | All | All | All |
| | 3.0 | All | All | All | All | All |
| | 4.0 | All | All | All | All | All |
| 100 | 1.1 | All | All | All | All | All |
| | 1.3 | All | All | All | All | All |
| | 1.5 | All | All | All | All | All |
| | 2.0 | All | All | All | All | All |
| | 3.0 | All | All | All | All | All |
| | 4.0 | All | All | All | All | All |
| 300 | 1.1 | All | All | All | All | All |
| | 1.3 | All | All | All | All | All |
| | 1.5 | All | All | All | All | All |
| | 2.0 | All | All | All | All | All |
| | 3.0 | All | All | All | All | All |
| | 4.0 | All | All | All | All | All |
| 500 | 1.1 | All | IWT p-chart | IWT $p$-chart | IWT $p$-chart | IWT p-chart |
| | 1.3 | All | IWT p-chart | IWT $p$-chart | IWT $p$-chart | IWT p-chart |
| | 1.5 | All | IWT p-chart | IWT $p$-chart | IWT $p$-chart | IWT p-chart |
| | 2.0 | All | IWT p-chart | IWT $p$-chart | IWT $p$-chart | IWT $p$-chart |
| | 3.0 | All | IWT $p$-chart | All | All | All |
| | 4.0 | All | IWT p-chart | All | All | All |
| 1000 | 1.1 | IWT p-chart | IWT p-chart | IWT $p$-chart | IWT $p$-chart | IWT p-chart |
| | 1.3 | IWT p-chart | IWT $p$-chart | IWT $p$-chart | IWT $p$-chart | IWT $p$-chart |
| | 1.5 | IWT p-chart | IWT p-chart | IWT $p$-chart | IWT p-chart | IWT p-chart |
| | 2.0 | IWT $p$-chart | IWT $p$-chart | IWT $p$-chart | All | All |
| | 3.0 | IWT p-chart | All | All | All | All |
| | 4.0 | IWT p-chart | All | All | All | All |

Note: Let "All" be the IWT $p$-chart, $p$-chart, ISRT $p$-chart and Wilson $p$-chart

**Practice** ***21***(4): 407–412. DOI: 10.1016/j.conengprac.2012.12.005.

[11] A. Duclos and N. Voirin, (2010) *"The p-control chart: a tool for care improvement"* **International Journal for Quality in Health Care** *22*(5): 402–407.

[12] S. Sukparungsee, (2014) *"An EWMA p chart based on improved square root transformation"* **International Journal of Physical and Mathematical Sciences** *8*(7): 1045–1047. DOI: 1307-6892/9998781.

[13] W. Rod-o, J. Sinsomboonthong, and T. Supapakorn, (2016) *"Quality control chart for monitoring the fraction nonconforming in production process for out-of-control process"* **Thai Science and Technology Journal**: 884–895. DOI: 10.14456/tstj.2016.72.

[14] G. Chen, (1998) *"An improved p chart through simple adjustments"* **Journal of Quality Technology** ***30***(2): 142–151. DOI: 10.1080/00224065.1998.11979833.

[15] T. R. Tsai, C. C. Lin, and S. J. Wu, (2006) *"Alternative attribute control charts based on improved square root transformation"* **Tamsui Oxford Journal of Mathematical Sciences** *22*(1): 61–72.

[16] H. Wang, (2009) *"Comparison of p control charts for low defective rate"* **Computational statistics and data analysis** *53*(12): 4210–4220.

**[17]** A. M. O. Anna and C. S. ten Caten, (2012) *"Beta control charts for monitoring fraction data"* **Expert Systems with Applications *39***(11): 10236–10243. DOI: 10.1016/j.eswa.2012.02.146.

**[18]** W. A. Shewhart. *Economic Control of Quality Manufacturing Product*. Van Nostrand Reinhold, Princeton, 1924.

**[19]** S. Rungruang, (2013) *"An efficiency comparison of fraction nonconforming control charts"* **Veridian E-Journal, Silpakorn University (Humanities, Social Sciences and arts) *6***(3): 860–876.

**[20]** A. Agresti and B. A. Coull, (1998) *"Approximate is better than "exact" for interval estimation of binomial proportions"* **The American Statistician *52***(2): 119–126.

**[21]** C. Park, (2013) *"An improved p chart based on the Wilson interval"* **Journal of Statistics and Management Systems *16***(2): 201–221. DOI: 10.1080/09720510.2013.777576.

**[22]** M. B. Khoo, S. Y. Teh, X. Chew, and W. L. Teoh, (2015) *"Standard deviation of the run length (SDRL) and average run length (ARL) performances of EWMA and synthetic charts"* **International Journal of Engineering and Technology *7***(6): 513–516.

**[23]** P. W. Chen, C. S. Cheng, and C. W. Wang, (2023) *"A Study on the Laney p control chart with parameters estimated from phase I data: performance evaluation and applications"* **Mathematics *11***(3411): 1–20. DOI: 10.3390/math11153411.

**[24]** S. K. Khilare and D. T. Shirke, (2023) *"The fraction nonconforming m-of-m control chart with warning limits"* **Thailand Statistician *21***(2): 435–449.

**[25]** M. Schader and F. Schmid, (1989) *"Two rules of thumb for the approximation of the binomial distribution by the normal distribution"* **The American Statistician *43***(1): 23–24. DOI: 10.1080/00031305.1989.10475601.

**[26]** C. H. Chang, J. J. Lin, N. Pal, and M. C. Chiang, (2008) *"A note on improved approximation of the binomial distribution by the skew-normal distribution"* **The American Statistician *62***(2): 167–170.

**[27]** M. F. A Saleh and D. S. Obeidat, (2022) *"Approximation of the binomial probability function uthe discrete normal distribution"* **International Journal of Statistics and Probability *11***(3): 32–39. DOI: 10.5539/ijsp.v11n3p32.

**[28]** S. I. Grossman. *Calculus*. Academic Press, 2014.

**[29]** T. Sincich. *Statistics by Example*. Macmillan, New York, 1993.

**[30]** N. A. Weiss. *Elementary Statistics*. Pearson, San Francisco, 2008.

**[31]** M. R. Aslam, R. A. Bantan, and N. Khan, (2019) *"Design of a new attribute control chart under neutrosophic statistics"* **International Journal of Fuzzy Systems *21***: 433–440. DOI: 10.1007/s40815-018-0577-1.